

Visible electroluminescence from hybrid colloidal silicon quantum dot-organic light-emitting diodes

Chang-Ching Tu,^{1,2,a)} Liang Tang,² Jiangdong Huang,² Apostolos Voutsas,² and Lih Y. Lin¹

¹Department of Electrical Engineering, University of Washington, Seattle, Washington 98195, USA

²Materials and Device Applications Laboratory, Sharp Laboratories of America, Inc., Camas, Washington 98607, USA

(Received 26 March 2011; accepted 3 May 2011; published online 23 May 2011)

We demonstrate hybrid colloidal silicon quantum dot (SiQD)-organic light-emitting diodes with electroluminescence (EL) in the visible wavelengths. The device using blue photoluminescence (PL) SiQDs as emitters shows multiple EL peaks which are attributed to carrier recombination in the core quantum confinement states, the hole-transport-layer and the surface trap states, respectively. However, the red PL SiQD device shows a single EL peak consistent with the PL peak. These findings are in agreement with the previous report that large Stokes shift were observed for oxidized blue emission SiQDs due to oxide states while red emission SiQDs show negligible PL shift after oxidation. © 2011 American Institute of Physics. [doi:10.1063/1.3593382]

Colloidal inorganic semiconductor quantum dots (QDs) with size-tunable band gaps, high photoluminescence (PL) quantum yield, and narrow emission line widths are a good candidate as solution-processable chromophores in a hybrid QD-organic light-emitting diode (QD-OLED) structure.¹⁻³ Visible electroluminescence (EL) from the hybrid structure has been reported in group II-VI semiconductor QD systems, such as CdSe, CdZnSe, ZnSe, or CdZnS cores with single or multiple shells.⁴⁻⁶ High luminance and high efficiency QD-OLEDs using these II-VI QDs have been recently demonstrated on a display with an active matrix drive backplane.^{7,8} Notably, heavy-metal-free ZnCuInS/ZnS core/shell QDs have also been employed in white emission OLEDs.⁹ However, for group IV colloidal semiconductor QDs, although there has been significant development in synthesis and characterization,¹⁰ the demonstration of visible EL from these nanomaterials is still under developing. Meanwhile, infrared-red group IV QD-OLEDs with promising efficiency have been recently reported.^{11,12} Silicon QDs (SiQDs) show tunable band gaps due to quantum confinement effect when the dot sizes are within the Bohr exciton radius of bulk Si (around 4.9 nm). Thus, visible, from red to blue, EL or PL can be achieved by adjusting QD radius from approximately 3.5 to 1.5 nm.¹³ Furthermore, compared to conventional II-VI QDs, SiQDs are heavy-metal-free, potentially compatible with well-established Si processing technologies and can be synthesized from almost inexhaustible starting materials in the earth crust. Here we demonstrate hybrid SiQD-OLEDs which show EL across the visible spectrum. By comparing devices using blue and red PL SiQDs as emissive layers, we identify the role of surface oxide states which limit the effective core quantum confinement band gap.

In this work, the SiQDs were synthesized by electrochemical etching of Si wafer, followed by surface passivation through hydrosilylation and ultrasonication for dispersing the QDs in solvents.¹⁴ In the electrochemical etching

reaction, we etched *p*-type boron-doped Si wafers with (100) orientation and 5–20 Ω cm resistivity under stirring in a mixture of hydrofluoric acid (HF), methanol, hydrogen peroxide (H₂O₂), and polyoxometalates (POMs), where the latter two ingredients function as catalysts.¹⁵ A mild etching recipe was used (etching current density=10 mA/cm², etching time=2 h, and small amount of H₂O₂) in order to avoid the formation of too many microsize pores on the wafer surface. After the electrochemical etching, the wafers were treated with diluted HF in a water/methanol mixture for further removal of oxide residues and the formation of purely hydride termination on the surface. Then, in a nitrogen filled glove box, the wafers were immersed in a hexane/1-octene mixture with a catalytic amount of chloroplatinic acid as catalysts for hydrosilylation reaction, where unsaturated double bonds of 1-octenes form stable covalent bonds with hydrides on the Si surface. With surface passivation by alkyl ligands, the wafers were ultrasonicated shortly in hexanes. The resulting nearly transparent suspension showed bright red PL under 350 nm UV excitation with a major peak at 612 nm and a smaller minor peak in the short wavelength region, as shown in Fig. 1(a). Passing the red PL suspension through a syringe filter (polypropylene membrane and pore size of 0.2 μm), we obtained a clear suspension of SiQDs

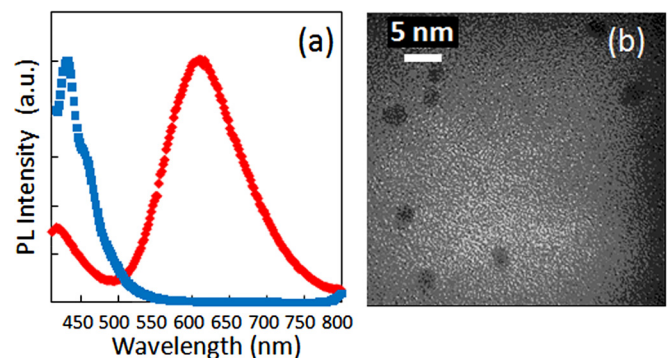


FIG. 1. (Color online) (a) The PL spectra of the blue (blue square line) and the red (red diamond line) emission SiQDs in hexanes. (b) The TEM image of the blue PL SiQDs.

^{a)}Author to whom correspondence should be addressed. Electronic mail: tucc@u.washington.edu.

which show blue PL with a narrow line width and a peak at 430 nm, as shown in Fig. 1(a). The transmission electron microscope (TEM) image of these blue PL SiQDs is shown in Fig. 1(b), from which the QD diameter of around 2 nm was estimated. The removal of the red peak by simply passing through the syringe filter is likely due to the following reasons: First, during the electrochemical etching, the red PL SiQDs were mostly formed on top of the microsize structures which were then dispersed into solvents together with SiQDs attached on the surface. Second, the red PL SiQDs tend to form aggregates and get retained when passing through pores of the syringe filter. Similar results have also been found in literature.^{16,17}

The multilayered light-emitting devices were composed of indium-tin-oxide (ITO)/poly(3,4-ethylenedioxythiophene):poly(styrenesulfonate) (PEDOT:PSS, 100 nm)/poly(*N,N'*-bis(4-butylphenyl)-*N,N'*-bis(phenyl) benzidine (poly-TPD, 50 nm)/SiQDs (around 5 nm in average thickness)/titanium dioxide (TiO₂, 65 nm)/Al (100 nm). First, the ITO substrates were sequentially cleaned by ultrasonication in de-ionized water, isopropanol, and acetone, and then treated with oxygen plasma for removing organic residues and enhancing surface hydrophilic property. The hole-injection-layer PEDOT:PSS (2.8 wt % dispersion in H₂O) was spin-coated at 4000 rpm for 40 s and baked in a nitrogen-filled glove box at 120 °C for 30 min. Subsequently, the hole-transport-layer poly-TPD (1.5 wt % in chlorobenzene) was spin-coated at 2000 rpm for 30 s and baked in the same glove box at 110 °C for 30 min. On the poly-TPD layer, the emissive layer of SiQDs (3 mg/ml in hexane for blue SiQDs and 10 mg/ml in hexane for red SiQDs) was spin-coated at 300 rpm for 30 s, followed by vacuum drying. For the electron-transport-layer, the TiO₂ precursor sol-gel was prepared (1.56 ml titanium isopropoxide in 12 ml 2-methoxyethanol) and spin-coated at 3000 rpm for 40 s, followed by heating at 80 °C in air. The moisture in air facilitated the precipitation and the formation of amorphous TiO₂ thin films. Finally, a thin film of Al was rf-sputtered through a shadow mask which defines the active area. Immediately after metallization, the QD-OLEDs were packaged with glass slides and high vacuum silicone grease. The following *I-V* curves and EL spectra measurements were performed in an ambient condition.

The energy band diagrams of the SiQD-OLEDs are illustrated in Figs. 2(a) and 4(a), with blue and red PL SiQDs as emissive layers, respectively. The energy levels of PEDOT:PSS, poly-TPD, and TiO₂ were taken from Refs. 11, 4, and 7, respectively. For blue emission SiQDs (PL peak at 430 nm), the quantum confinement energy is estimated to be ~1.77 eV, from which ~0.59 eV is assigned to conduction band (CB) and ~1.18 eV to is assigned to valence band (VB).¹⁸ Similarly for red emission SiQDs (PL peak at 612 nm), ~0.30 eV and ~0.61 eV are assigned to CB and VB, respectively. The EL spectra of the blue SiQD-OLED are shown in Fig. 2(b) at current density=34.6, 46.2, 57.7, and 69.3 mA/cm². We observed the optical power increased almost linearly as the current density increased, and the *I-V* curve followed a typical diode rectifying characteristic, as shown in Fig. 3(a). At the highest input current density in Fig. 2(b) (69.3 mA/cm²), the optical power density of the blue SiQD-OLED was measured to be around 150 nW/cm²

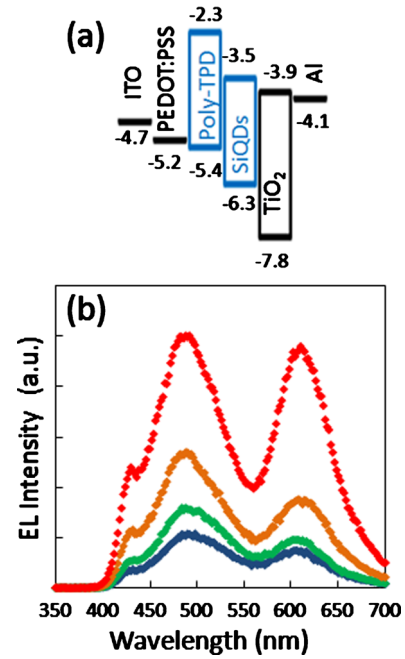


FIG. 2. (Color online) (a) The energy band diagram of the blue emission SiQD-OLED. (b) The EL spectra of the blue emission SiQD-OLED at current density=34.6 (bottom, blue line), 46.2 (lower middle, green line), 57.7 (upper middle, orange line), and 69.3 (top, red line) mA/cm².

which corresponds to an external quantum efficiency of around $1 \times 10^{-5}\%$.

In the EL spectra of Fig. 2(b), we also observed that there were three peaks at all current densities, which are 430, 488, and 606 nm. The 430 nm EL peak, consistent with the blue PL peak in Fig. 1(a), is likely due to carrier recombination in the core quantum confinement states of the blue emission SiQDs. Then, we measured the thin film PL spectrum of a reference device (ITO/PEDOT:PSS/poly-TPD) and observed a peak at 486 nm as shown in Fig. 3(b). As a result, the 488 nm EL peak can be attributed to carrier recombination in the poly-TPD layer. For the orangish 606 nm peak, it is likely due to carrier recombination through the surface trap states of the oxidized blue emission SiQDs. The oxidation might occur when the device was heated in air after TiO₂ coating and/or during the EL measurement. The trap states located in the energy band gap lower the radiative recombination energy and thus shift the emission toward longer wavelengths. Similar results were found in a PL study of SiQDs on porous silicon surface prepared by electrochemical etching of *p*-type Si wafers.¹⁹ In their findings, upon oxida-

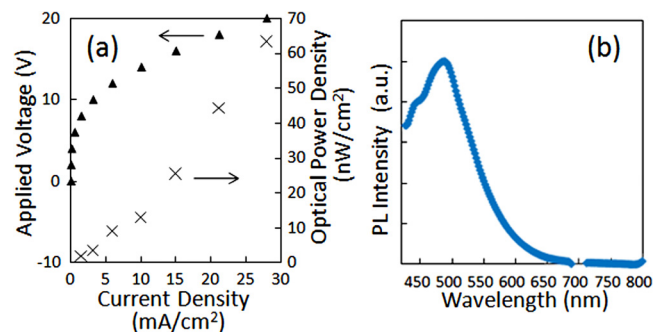


FIG. 3. (Color online) (a) The applied voltage (triangle line) and the optical power density (cross line) of the blue emission SiQD-OLED. (b) The thin film PL spectrum of a reference device with structure of ITO/PEDOT:PSS/poly-TPD.

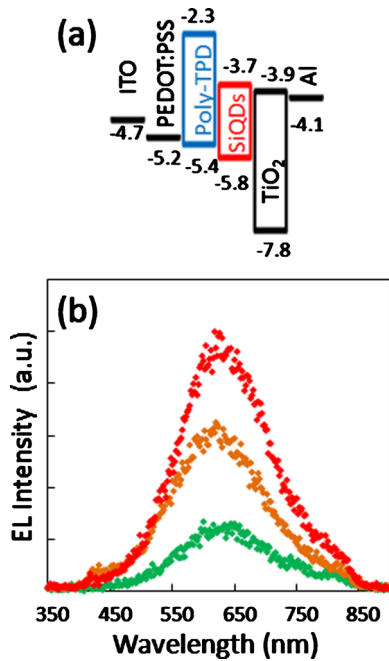


FIG. 4. (Color online) (a) The energy band diagram of the red emission SiQD-OLED. (b) The EL spectra of the red emission SiQD-OLED at current density=46.2 (bottom, green line), 69.3 (middle, orange line), and 115.5 (top, red line) mA/cm².

tion SiQDs with blue or green PL showed a large Stokes shift and the upper limit of the emission energy was 2.1 eV (590 nm) due to localized states in the Si=O bonds, which is close to the 606 nm observed in our EL measurement. However, for the SiQDs which display orange or red emission, the oxide states have a negligible impact on the PL spectrum according to their results.¹⁹

In order to verify the role of oxygen in red emission SiQDs and observe their EL response, we fabricated another QD-OLED with the same structure but using red PL SiQDs [PL spectrum in Fig. 1(a)] as the emissive layer. The energy band structure and the EL spectra at current density=46.2, 69.3, and 115.5 mA/cm² of the red SiQD-OLED are in Figs. 4(a) and 4(b), respectively. First, the *I-V* characteristics were similar to the blue SiQD-OLED. However, the quantum efficiency was about 15 times lower as a result of not only nanocrystalline SiQDs but also some microsize Si particles being embedded in the emissive layer. The microsize particles generate no EL but can absorb the emission from SiQDs. In contrast, the blue emission SiQD suspension had purely nanosize particles due to filtration through a syringe filter. Second, the EL peak at 618 nm is close to the red SiQD PL peak at 612 nm. Therefore, the orangish EL should come from carrier recombination in the core quantum confinement states of SiQDs, considering poly-TPD has only blue emission. Furthermore, since the energy band gap of red SiQDs (612 nm) is smaller than the energy difference between electron and hole trap states (590 nm), the oxide states had negligible effect on the EL or PL spectra. Consequently, we observed only one EL peak at 618 nm, rather than multiple peaks as for the blue Si QD-OLED. Finally, at the poly-TPD/SiQDs interface, the CB energy barrier of the red SiQD-OLED (1.4 eV) is larger than that of the blue SiQD-OLED

(1.2 eV) and the VB energy barrier of the red SiQD-OLED (0.4 eV) is smaller than that of the blue SiQD-OLED (0.9 eV). Therefore, there is better electron-stop and hole-transport at the poly-TPD/SiQDs interface, which leads to much less carrier recombination in the poly-TPD layer for the red SiQD-OLED.

In conclusion, we have demonstrated hybrid colloidal SiQD-OLEDs with EL in the visible wavelengths. The SiQDs were synthesized by electrochemical etching of Si wafers, followed by alkyl-ligand passivation through hydrosilylation and ultrasonication for dispersing SiQDs. The device with blue PL SiQDs showed multiple EL peaks which are attributed to carrier recombination in the core quantum confinement states, the poly-TPD and the surface trap states due to oxidation, respectively. In contrast, the red PL SiQD device showed a single EL peak consistent with the PL peak. These findings are in good agreement with the previous PL study of SiQDs on the porous Si surface.

This project was supported in part by the National Science Foundation (Grant No. ECCS-0925378 and the supplementary GOALI grant). Work was performed in part at the University of Washington, Nanotech User Facility (NTUF), a member of the National Nanotechnology Infrastructure Network (NNIN), which is supported by the National Science Foundation.

- ¹V. L. Colvin, M. C. Schlamp, and A. P. Alivisatos, *Nature (London)* **370**, 354 (1994).
- ²S. Coe, W.-K. Woo, M. Bawendi, and V. Bulovic, *Nature (London)* **420**, 800 (2002).
- ³S. Coe-Sullivan, W.-K. Woo, J. S. Steckel, M. Bawendi, and V. Bulovic, *Org. Electron.* **4**, 123 (2003).
- ⁴W. K. Bae, J. Kwak, J. W. Park, K. Char, C. Lee, and S. Lee, *Adv. Mater. (Weinheim, Ger.)* **21**, 1690 (2009).
- ⁵W. K. Bae, J. Kwak, J. Lim, D. Lee, M. K. Nam, K. Char, C. Lee, and S. Lee, *Nanotechnology* **20**, 075202 (2009).
- ⁶Y.-H. Niu, A. M. Munro, Y.-J. Cheng, Y. Tian, M. S. Liu, J. Zhao, J. A. Bardecker, I. J.-L. Plante, D. S. Ginger, and A. K.-Y. Jen, *Adv. Mater. (Weinheim, Ger.)* **19**, 3371 (2007).
- ⁷K.-S. Cho, E. K. Lee, W.-J. Joo, E. Jang, T.-H. Kim, S. J. Lee, S.-J. Kwon, J. Y. Han, B.-K. Kim, B. L. Choi, and J. M. Kim, *Nat. Photonics* **3**, 341 (2009).
- ⁸E. Jang, S. Jun, H. Jang, J. Lim, B. Kim, and Y. Kim, *Adv. Mater. (Weinheim, Ger.)* **22**, 3076 (2010).
- ⁹Y. Zhang, C. Xie, H. Su, J. Liu, S. Pickering, Y. Wang, W. W. Yu, J. Wang, Y. Wang, J.-i. Hahn, N. Dellas, S. E. Mohney, and J. Xu, *Nano Lett.* **11**, 329 (2011).
- ¹⁰J. G. C. Veinot, *Chem. Commun. (Cambridge)* **2006**, 4160.
- ¹¹K.-Y. Cheng, R. Anthony, U. R. Kortshagen, and R. J. Holmes, *Nano Lett.* **10**, 1154 (2010).
- ¹²D. P. Puzzo, E. J. Henderson, M. G. Helander, Z. Wang, G. A. Ozin, and Z. Lu, *Nano Lett.* **11**, 1585 (2011).
- ¹³J. P. Poot, C. Delerue, and G. Allan, *Appl. Phys. Lett.* **61**, 1948 (1992).
- ¹⁴C.-C. Tu, L. Tang, J. Huang, A. Voutsas, and L. Y. Lin, *Opt. Express* **18**, 21622 (2010).
- ¹⁵Z. Kang, C. H. A. Tsang, Z. Zhang, M. Zhang, N.-B. Wong, J. A. Zapien, Y. Shan, and S.-T. Lee, *J. Am. Chem. Soc.* **129**, 5326 (2007).
- ¹⁶R. A. Bley, S. M. Kauzlarich, J. E. Davis, and H. W. H. Lee, *Chem. Mater.* **8**, 1881 (1996).
- ¹⁷G. Belomoin, J. Therrien, and M. Nayfeh, *Appl. Phys. Lett.* **77**, 779 (2000).
- ¹⁸T. van Buuren, L. N. Dinh, L. L. Chase, W. J. Siekhaus, and L. J. Terminello, *Phys. Rev. Lett.* **80**, 3803 (1998).
- ¹⁹M. V. Wolkin, J. Jorne, P. M. Fauchet, G. Allan, and C. Delerue, *Phys. Rev. Lett.* **82**, 197 (1999).